Electronic Supplementary Material (ESI) for Journal of Materials Chemistry A.


# Supporting information

## Effect of Composition and Nanostructuring of Palladium Selenides, $Pd_4Se$, $Pd_7Se_4$ and $Pd_{17}Se_{15}$ on Oxygen Reduction Activity and Their use in Mg-Air Batteries

Suresh Kukunuri, Keerti Naik, S. Sampath*

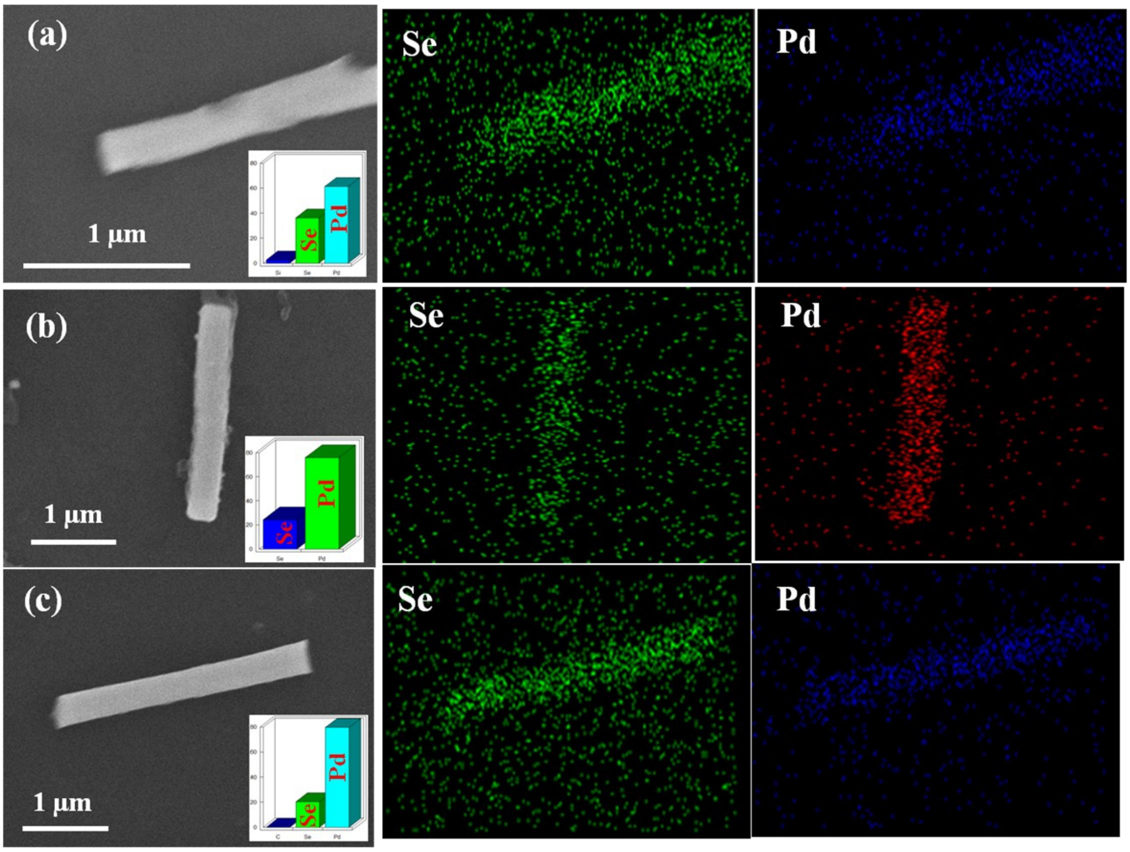


**Figure S1.** SEM images and corresponding elemental mapping of (a) $Pd_{17}Se_{15}$, (b) $Pd_7Se_4$ and (c) $Pd_4Se$ [mapping images indicates the presence of Se and Pd in all the three nanostructures and inset in a, b and c indicates the respective weight percentages of Pd and Se from EDAX analysis].

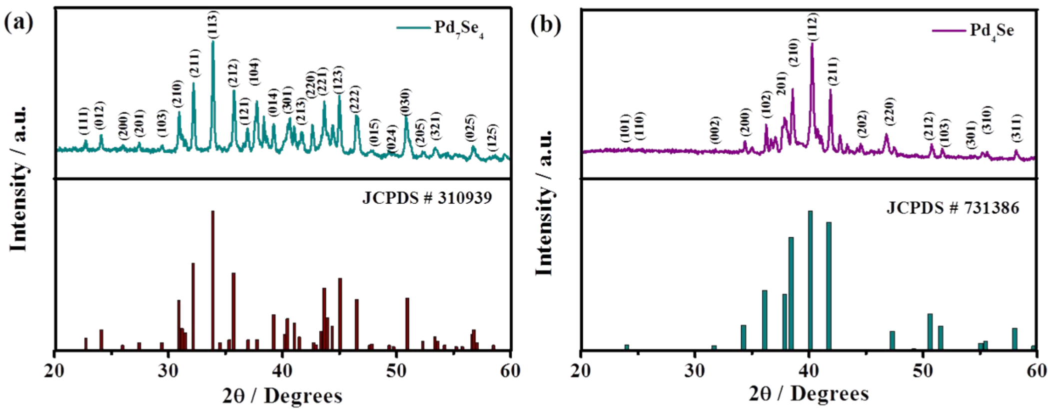


Fig S2. XRD patterns of $Pd_7Se_4$ (a) and $Pd_4Se$ (b) nanostructures prepared on AAO template.

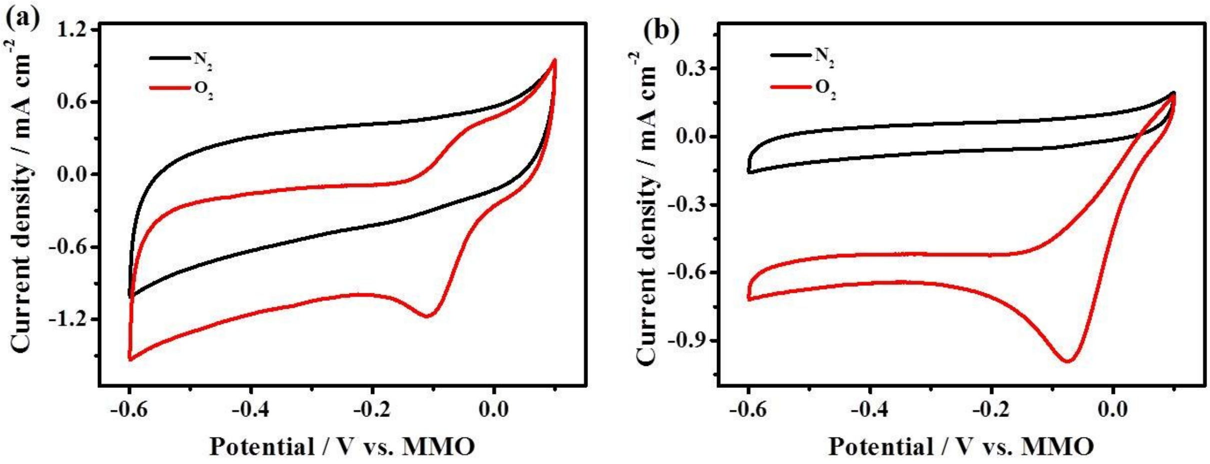


**Figure S3.** Cyclic voltammograms of (a) $Pd_7Se_4$ and (b) $Pd_4Se$ in the presence of $N_2$ and $O_2$ in 0.1 M KOH solution at a scan rate of 50 $mVs^{-1}$.

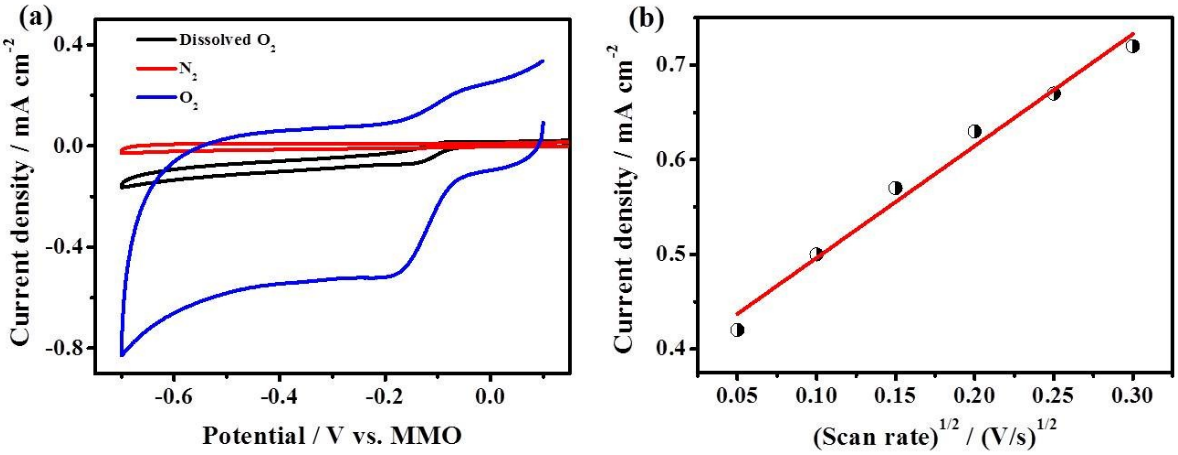


**Figure S4.** (a) Cyclic voltammograms of $Pd_{17}Se_{15}$ in $N_2$-saturated, $O_2$-saturated and in the presence of dissolved $O_2$, (b) Variation of peak current density as a function of square root of scan rate on $Pd_{17}Se_{15}$ in $O_2$-saturated 0.1 M KOH solution.

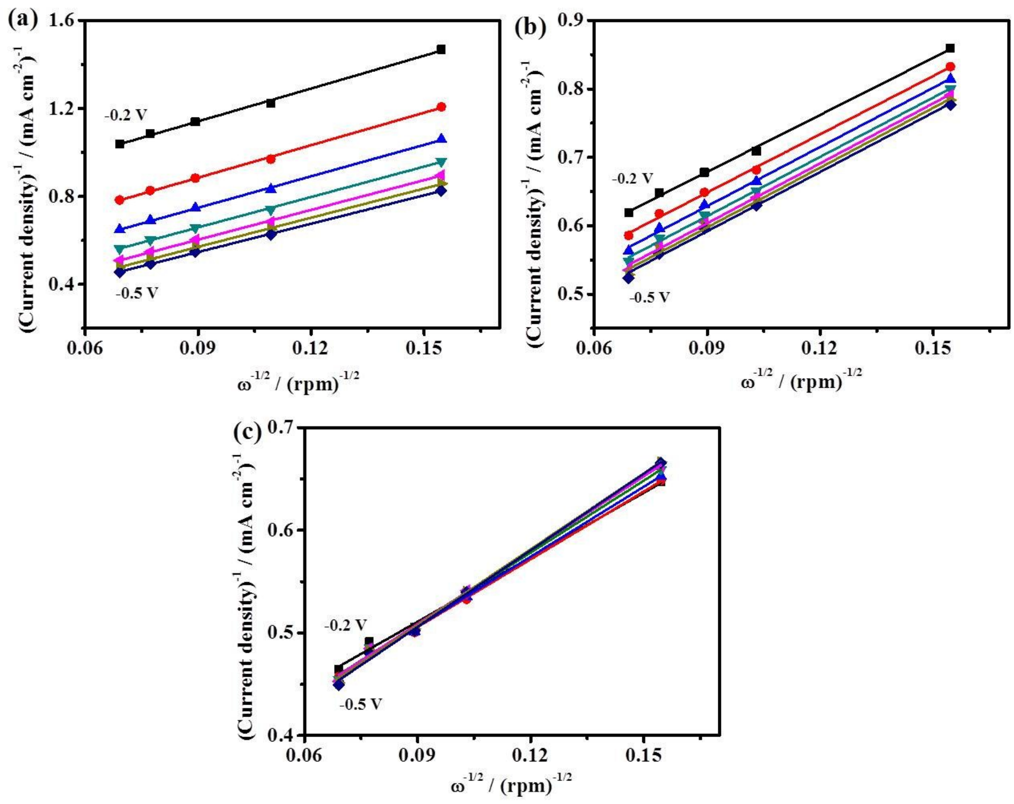

**Figure S5.** K-L plots at different potentials from -0.2 to -0.5 V in the interval of -0.05 V on $Pd_{17}Se_{15}$, $Pd_7Se_4$ and $Pd_4Se$ recorded at a scan rate of 2 $mVs^{-1}$.

**Determination of kinetic parameters**

The kinetic parameters such as rate constant, kinetic current density and number of electrons transferred during $O_2$ reduction are extracted from the voltammograms at different potentials and at different rotation speeds using Koutecky-Levich (K-L) equation as given below **(equation 1)**.

$$\frac{1}{i} = \frac{1}{i_k} + \frac{1}{B\omega^{1/2}} \tag{1}$$

where i is the measured current, $i_k$ is the kinetic current and ω is the electrode rotating rate. The value of Levich slope (B) is evaluated from the following **equation 2**.

$$B = 0.62nFC_{O_2}D_{O_2}^{2/3}\upsilon^{-1/6} \tag{2}$$

where n indicates the transferred electrons number per $O_2$ molecule, F is the Faraday constant (F = 96485 C $mol^{-1}$), $C_{O_2}$ is the concentration of $O_2$ in the electrolyte ($C_o = 1.2 \times 10^{-6}$ $molm^{-3}$) $D_{O_2}$ is the diffusion coefficient of $O_2$ ($D_o = 1.9 \times 10^{-5}$ $cm^2$ $s^{-1}$), and υ is the kinematic viscosity (υ = 0.01 $cm^2$ $s^{-1}$).[40]

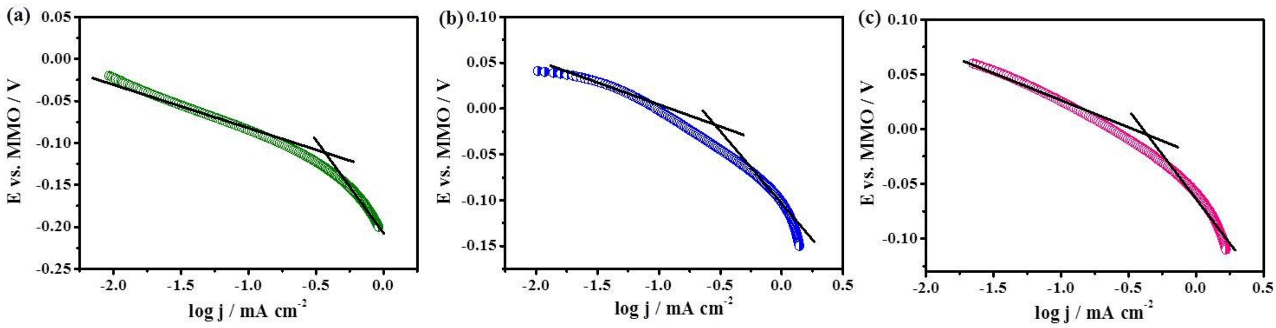


**Figure S6.** Tafel plots for ORR on (a) $Pd_{17}Se_{15}$, (b) $Pd_7Se_4$ and (c) $Pd_4Se$ in $O_2$-saturated 0.1 M KOH with a scan rate of 2 $mVs^{-1}$.

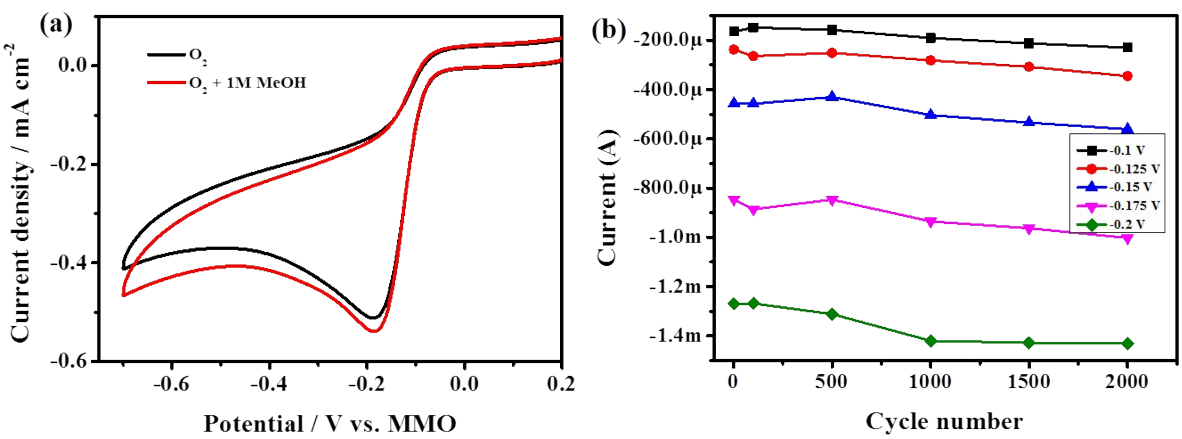

**Figure S7.** (a) Cyclic voltammograms for ORR in absence (black) and in presence (red) of 1 M methanol on $Pd_{17}Se_{15}$ catalyst. Supporting electrolyte used is 0.1 M KOH with a sweep rate of 50 $mVs^{-1}$, (b) Retention of current vs. cycle number at different applied potentials (Supporting electrolyte is $O_2$ saturated 0.1 M KOH and scan rate of 100 $mVs^{-1}$).

**Different environments present around Pd**

**$Pd_{17}Se_{15}$**

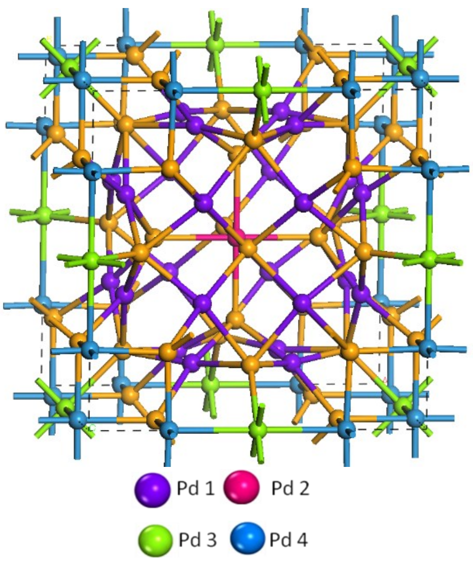


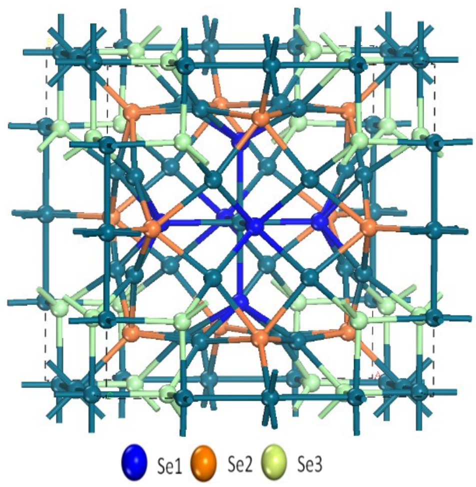


**$Pd_7Se_4$**

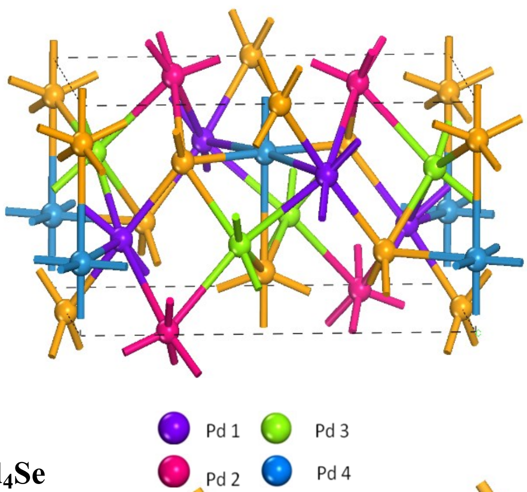


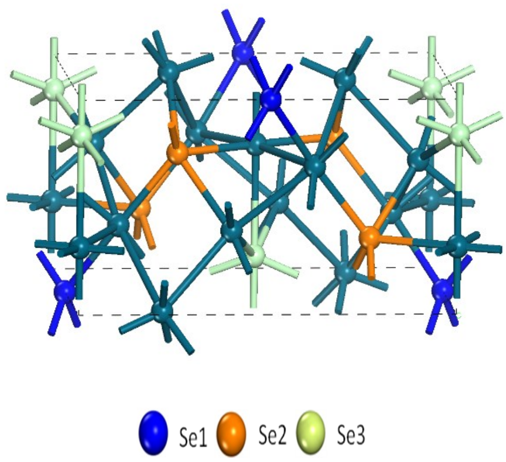


**$Pd_4Se$**

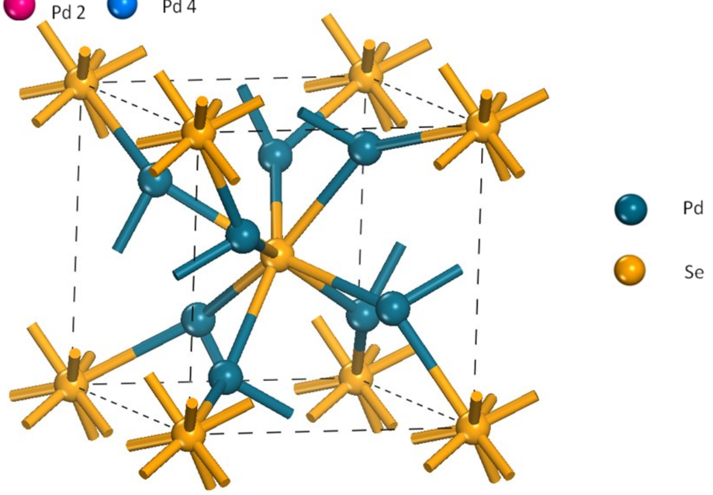

**Figure S8.** Different environment present around palladium in the three different phases, $Pd_{17}Se_{15}$, $Pd_7Se_4$ and $Pd_4Se$.

**Table S1.** Variation of rate constant values at different potentials on $Pd_{17}Se_{15}$ bulk and nanostructures.

| Potential (V) | $Pd_{17}Se_{15}$ (bulk) / cm $sec^{-1}$ | $Pd_{17}Se_{15}$ (nanorods) / cm $sec^{-1}$ |
|---|---|---|
| -0.2 | $8.4 \times 10^{-3}$ | $2.3 \times 10^{-2}$ |
| -0.3 | $1.1 \times 10^{-2}$ | $2.8 \times 10^{-2}$ |
| -0.4 | $1.3 \times 10^{-2}$ | $3.1 \times 10^{-2}$ |
| -0.5 | $1.5 \times 10^{-2}$ | $3.5 \times 10^{-2}$ |

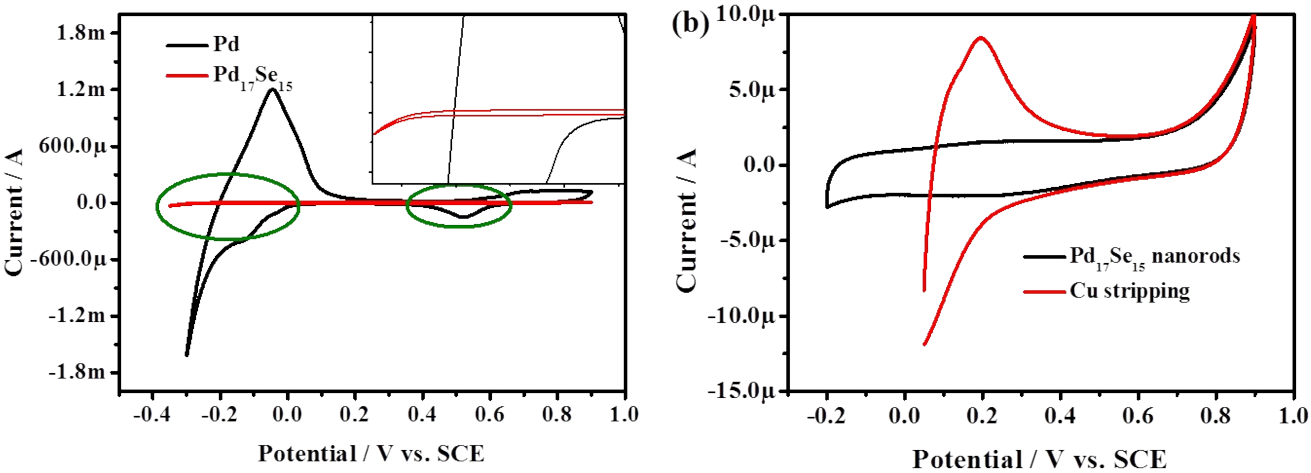


**Figure S9.** Cyclic voltammograms of Pd and $Pd_{17}Se_{15}$ on a glassy-carbon disk electrode in $N_2$-saturated 0.5 M $H_2SO_4$ with scan rate of 50 $mVs^{-1}$. [circled region indicates the absence of oxidation of palladium in $Pd_{17}Se_{15}$ which is also shown in the inset]. Cu under potential deposition (UPD) stripping voltammograms on (b) $Pd_{17}Se_{15}$ nanorods in 0.5 M $H_2SO_4$ + 2 mM $CuSO_4$ saturated with nitrogen at a sweep rate of 10 mV/s. Respective background voltammograms at the same scan rate without $CuSO_4$ are also shown.

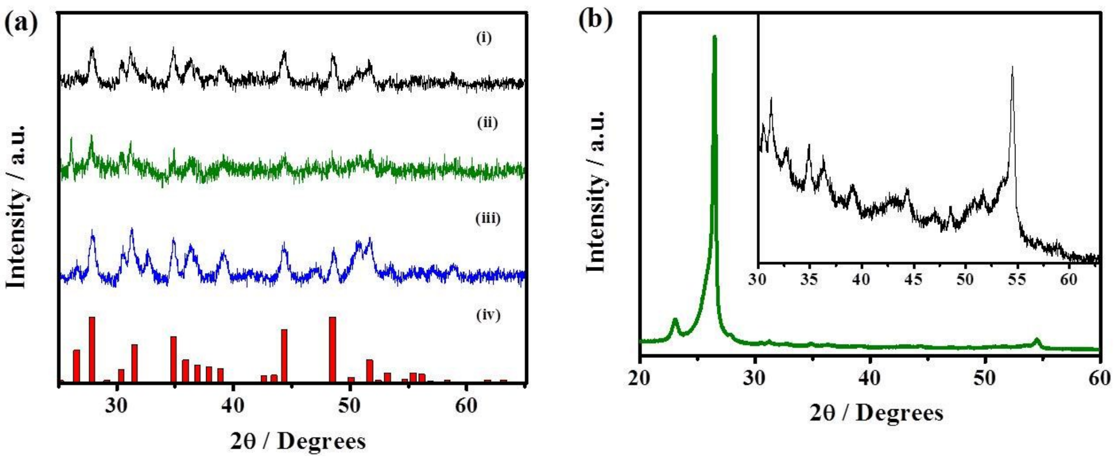

**Figure S10.** (a) XRD patterns of $Pd_{17}Se_{15}$ powder (i), acetylene black-$Pd_{17}Se_{15}$ (ii), rGO-$Pd_{17}Se_{15}$ (iii) and the standard pattern of $Pd_{17}Se_{15}$ (iv) and (b) XRD pattern of $Pd_{17}Se_{15}$ on toray carbon. [Inset shows the enlarged region from 30 to 60º]

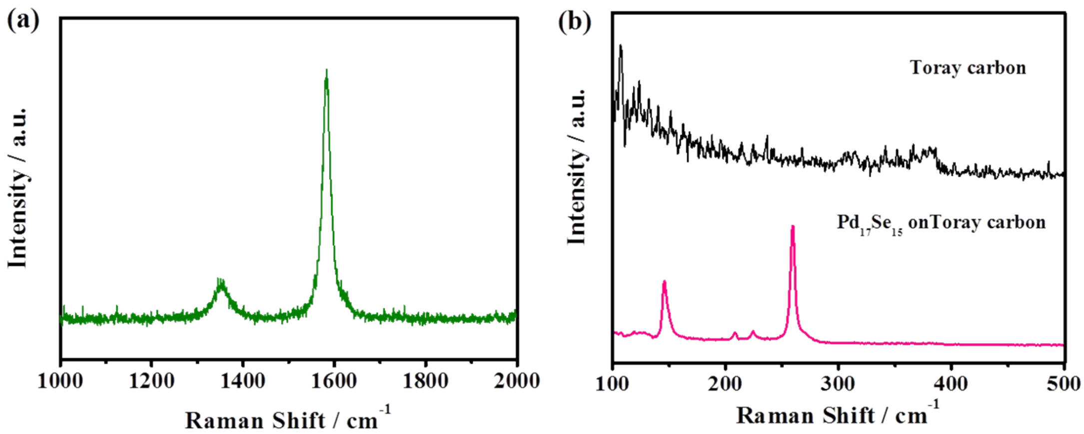


**Figure S11.** Raman spectra of (a) Toray carbon and (b) only toray carbon and $Pd_{17}Se_{15}$ supported on toray carbon.

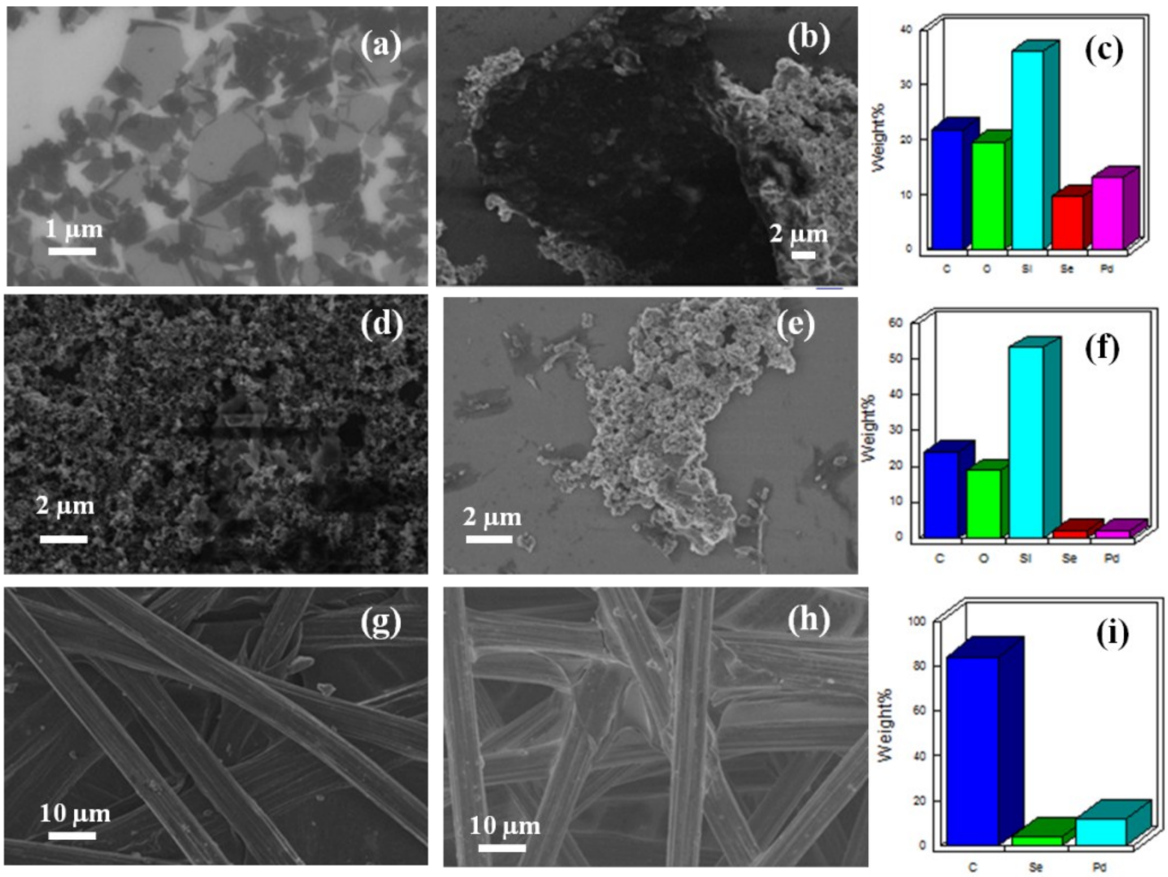


**Figure S12.** SEM images of (a) GO, (b) GO-$Pd_{17}Se_{15}$, (d) acetylene black, (e) acetylene black-$Pd_{17}Se_{15}$, (g) toray carbon, (h) toray carbon-$Pd_{17}Se_{15}$ and (c), (f) & (i) are the corresponding EDAX images of the composites.

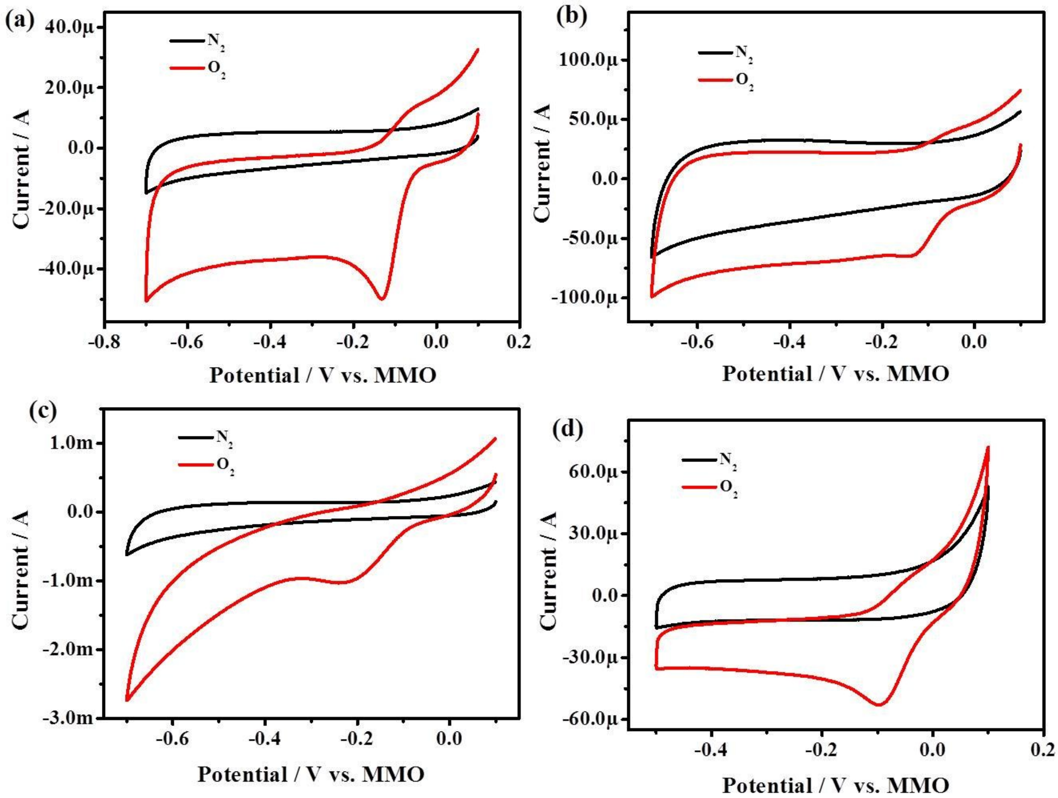


**Figure S13.** Cyclic voltammograms of (a) $Pd_{17}Se_{15}$-acetylene black, (b) $Pd_{17}Se_{15}$-reduced graphene oxide, (c) $Pd_{17}Se_{15}$-toray carbon and (d) $Pd_{17}Se_{15}$ nanostructures in $N_2$ and $O_2$-saturated 0.1 M KOH solution.

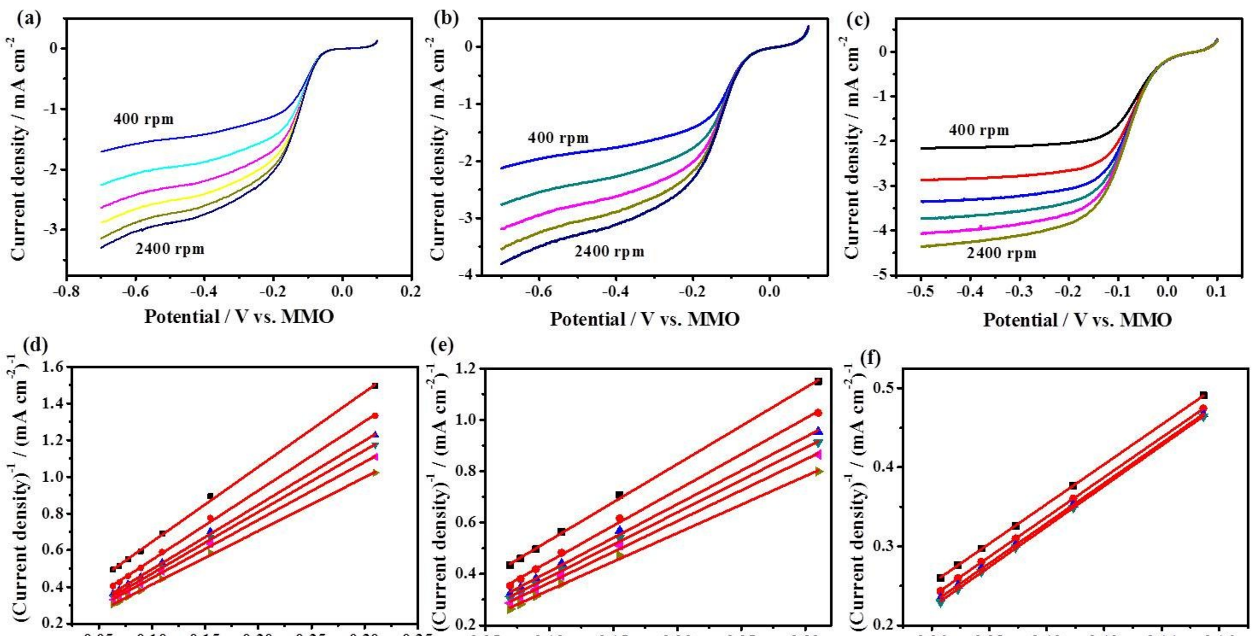


**Figure S14.** Linear sweep voltammograms of (a) $Pd_{17}Se_{15}$-acetylene black, (b) $Pd_{17}Se_{15}$-reduced graphene oxide, (c) $Pd_{17}Se_{15}$ nanostructures in $O_2$-saturated 0.1 M KOH at scan rate of 2 $mVs^{-1}$ at different rotation rates from 400 to 2400 rpm in the interval of 400 and (d), (e) & (f) corresponding K-L plots at different potentials vs. MMO.

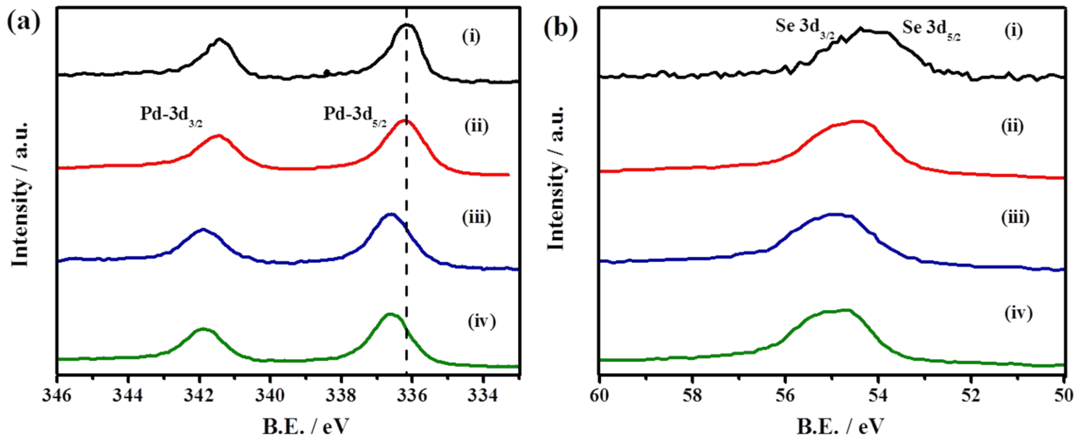


**Figure S15.** XPS spectra of (a) Pd-3d and (b) Se-3d for (i) $Pd_{17}Se_{15}$, (ii) acetylene black-$Pd_{17}Se_{15}$, (iii) rGO-$Pd_{17}Se_{15}$ and (iv) toray carbon-$Pd_{17}Se_{15}$.

**Table S2:** Binding energy values of Pd-3d and Se-3d levels in different carbon composite materials.

| Material | Pd-3d$_{5/2}$ (eV) | Pd-3d$_{3/2}$ (eV) | Se-3d$_{5/2}$ (eV) | Se-3d$_{5/2}$ (eV) |
|---|---|---|---|---|
| $Pd_{17}Se_{15}$ | 336.1 | 341.3 | 53.8 | 54.7 |
| rGO-$Pd_{17}Se_{15}$ | 336.2 | 341.4 | 54.2 | 54.9 |
| AB-$Pd_{17}Se_{15}$ | 336.5 | 341.8 | 54.5 | 55.4 |
| TC-$Pd_{17}Se_{15}$ | 336.6 | 341.9 | 54.6 | 55.5 |

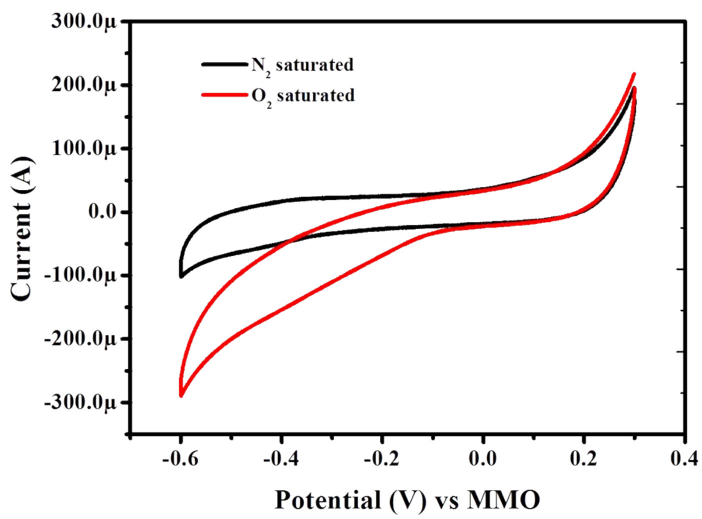


**Figure S16.** Cyclic voltammograms recorded in 2.6 M $Mg(NO_3)_2$ + 3.6 M $NaNO_2$ at a scan rate of 100 $mVs^{-1}$ in $O_2$ and $N_2$ saturated conditions.

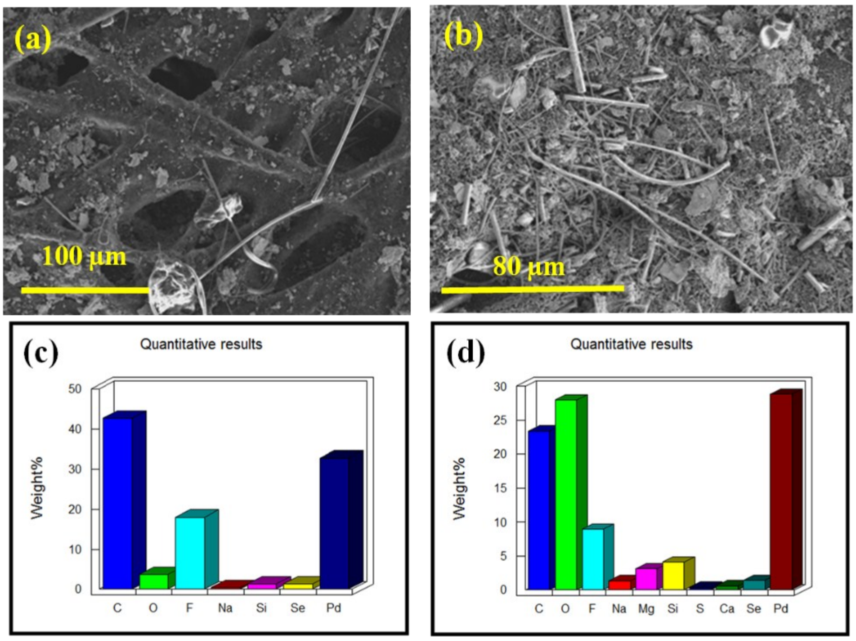


**Figure S17.** SEM images of $Pd_4Se$ (a) before [(c) presence of Pd and Se] and (b) after discharge [(d) presence of Pd and Se along with increased oxygen content] of Mg-air battery.

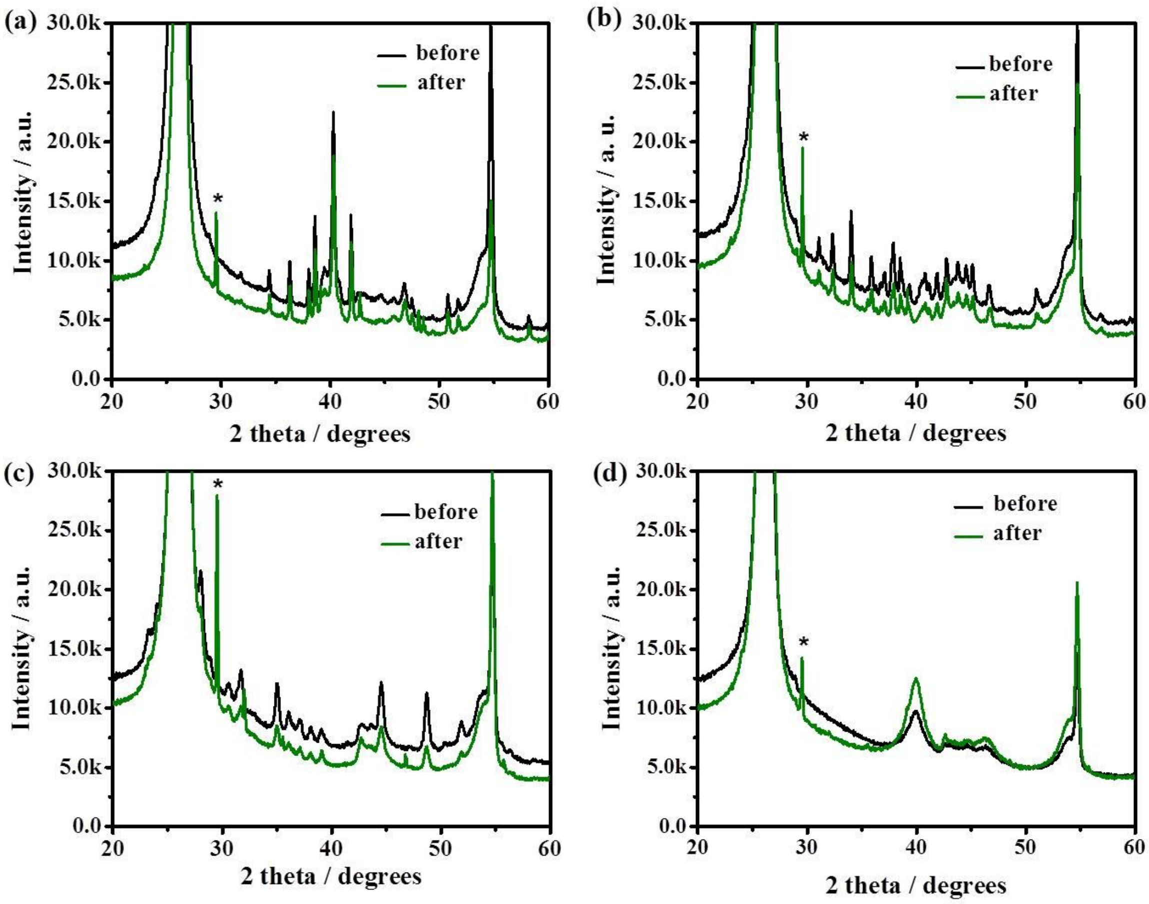


**Figure S18.** XRD patterns of (a) $Pd_4Se$ (b) $Pd_7Se_4$, (c) $Pd_{17}Se_{15}$ and (d) Pt, before and after discharge of Mg-air primary batteries.

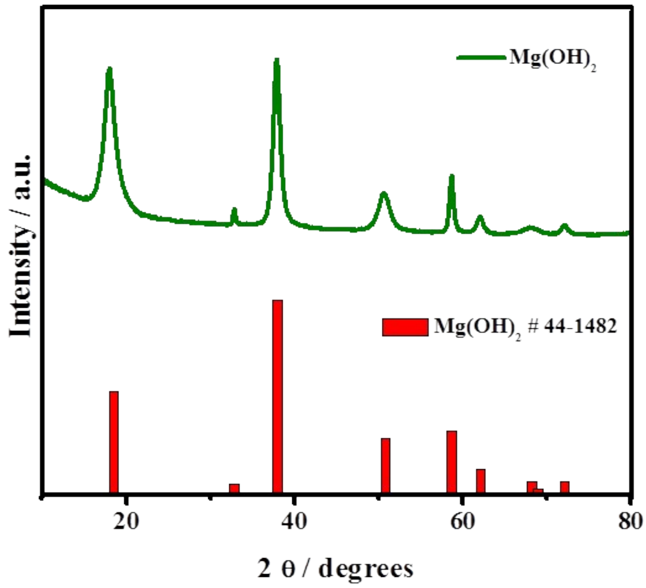


**Figure S19.** XRD pattern and the corresponding standard pattern of $Mg(OH)_2$ formed on the Mg foil after battery discharge.

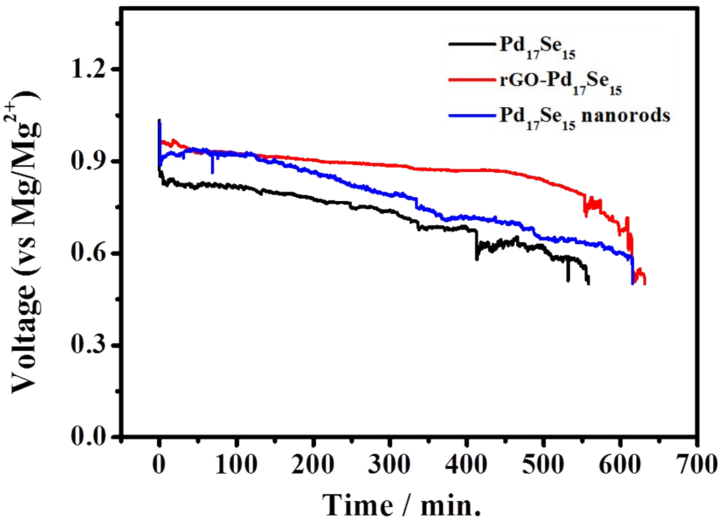


**Figure S20.** Discharge curves of Mg-$O_2$ battery with bulk $Pd_{17}Se_{15}$, $Pd_{17}Se_{15}$ supported on rGO and $Pd_{17}Se_{15}$ nanorods as cathodes. Constant current density of 1 mA $cm^{-2}$ is used for discharge.

**Table S3:** Comparison of discharge capacity values of palladium selenides with other reported catalysts in literature.

| Anode | Cathode | Electrolyte | Operating Voltage (V) | Discharge capacity (mAh $g^{-1}$) | References |
|---|---|---|---|---|---|
| AMX602 and AM60 alloys | Activated carbon sheet | 5 mass% NaCl | ~ 0.65 | 1331 | *J. Power Sources*, **2015**, *297*, 449 |
| **Mg foil** | **Ag** | **Organic/Aqueous** | **~ 0.8** | **2020** | ***J. Power Sources*, 2014, *247*, 840** |
| Mg-Li-Al-Ce alloy | Silver | 3.5 wt % NaCl | ~ 1.27 | 2072 | *J. Power Sources*, **2011**, *196*, 2346 |
| Mg piece | Pt/C, Pt–Mo/C | 3.5 wt % NaCl | ~ 1.3 | 1311 | *RSC Adv.*, **2016**, *6*, 83025 |
| Mg nano/ micro spheres | γ-$MnO_2$ | 2.6 M $Mg(NO_3)_2$ + 3.6 M $NaNO_2$ | ~ 1.5 | 768 | *Nano Research*, **2009**, *2*, 713 |
| **Mg micro particles** | **$Pd_4Se$** | **2.6 M $Mg(NO_3)_2$ + 3.6 M $NaNO_2$** | **~ 0.9** | **2228** | **Present work** |